THE JOURNAL OF PHYSICAL CHEMISTRY LETTERS
A JOURNAL OF THE AMERICAN CHEMICAL SOCIETY

pubs.acs.org/JPCL
Letter

Pulse Dipolar Electron Paramagnetic Resonance Spectroscopy Distance Measurements at Low Nanomolar Concentrations: The Cu^{II}-Trityl Case

Katrin Ackermann, Caspar A. Heubach, Olav Schiemann,* and Bela E. Bode*

Cite This: *J. Phys. Chem. Lett.* 2024, 15, 1455−1461
Read Online

ABSTRACT: Recent sensitivity enhancements in pulse dipolar electron paramagnetic resonance spectroscopy (PDS) have afforded distance measurements at submicromolar spin concentrations. This development opens the path for new science as more biomolecular systems can be investigated at their respective physiological concentrations. Here, we demonstrate that the combination of orthogonal spin-labeling using Cu^{II} ions and trityl yields a >3-fold increase in sensitivity compared to that of the established Cu^{II}-nitroxide labeling strategy. Application of the recently developed variable-time relaxation-induced dipolar modulation enhancement (RIDME) method yields a further ∼2.5-fold increase compared to the commonly used constant-time RIDME. This overall increase in sensitivity of almost an order of magnitude makes distance measurements in the range of 3 nm with protein concentrations as low as 10 nM feasible, >2 times lower than the previously reported concentration. We expect that experiments at single-digit nanomolar concentrations are imminent, which have the potential to transform biological PDS applications.

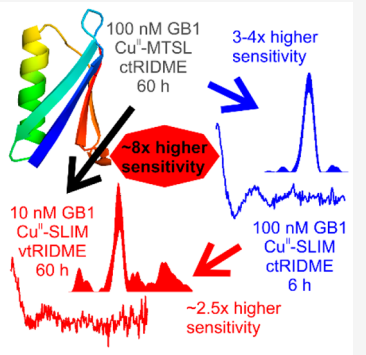

Studying the structure−function relationship of proteins and their complexes under physiological conditions is a major task for our understanding of the biomolecular mechanisms underpinning health and disease. However, the high concentration sensitivity required to meet physiologically relevant conditions pushes many biophysical methods, especially magnetic resonance techniques, to or even beyond their sensitivity limits. In this Letter, we demonstrate that distance measurements based on pulse dipolar electron paramagnetic resonance spectroscopy (PDS) can be performed at the required low nanomolar protein concentrations. This becomes possible by combining recent developments in pulse sequences with new labeling techniques.

Recent developments in electron paramagnetic resonance (EPR) spectroscopy have firmly established PDS in the toolbox for structural biology, due to its accuracy, reproducibility, and concentration sensitivity, and by providing access to full conformational ensembles of biomolecules.[1−6] PDS methods such as pulsed electron−electron double resonance (PELDOR or DEER),[7−9] relaxation-induced dipolar modulation enhancement (RIDME),[10−14] and double quantum coherence (DQC)[1,3,15] provide distance distributions in the nanometer range (from ∼2 to ∼16 nm)[16−18] and have become important tools for studying complex biomolecular systems.[19,20]

PDS requires the presence of paramagnetic centers that are dipolarly coupled; distance distributions can then be derived from the dipolar coupling frequencies. The beauty of this technique is that PDS is exquisitely and exclusively sensitive to these paramagnetic centers, such that the size, shape, and complexity of the overall biomolecular assembly are not considered limiting factors, allowing studies of proteins, nucleic acids, and their complexes *in vitro* and in cell.[2,18,21−32]

In most cases, paramagnetic centers are introduced via site-directed spin-labeling (SDSL) of specific residues, usually employing stable organic radicals such as nitroxides[1,33−35] or trityls[3,23,36] or paramagnetic metal ions such as Gd^{III},[21,34,36−39] Mn^{II},[40] or Cu^{II}.[41−44] In most cases, SDSL involves stable radicals introduced via cysteine-specific chemistry, where the label-specific length of the linker contributes degrees of freedom to the dynamics of the protein, which artificially broadens distance distributions or allows only distinct label conformations that could make interpretation of distance distributions ambiguous.[45,46] Additionally, different spin-labels may lead to different degrees of perturbation of the native structure due to their size and interactions with protein residues, e.g., trityl labels. Another approach uses Cu^{II} complexed with nitrilotriacetic acid (CuNTA) coordinated to a site-specifically introduced double-histidine (dHis) motif (dHis-CuNTA), posing more stringent requirements on the labeling site but yielding very narrow distance distributions due

Received: November 24, 2023
Revised: January 11, 2024
Accepted: January 19, 2024

https://doi.org/10.1021/acs.jpclett.3c03311
J. Phys. Chem. Lett. 2024, 15, 1455−1461

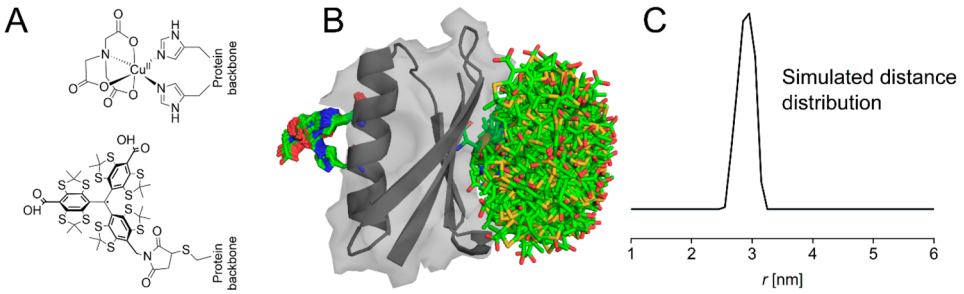

Figure 1. Predicted spatial distribution of the SLIM label and dHis-CuNTA in the GB1 construct I6SLIM/K28H/Q32H, based on the crystal structure of Protein Data Bank entry 4WH4. (A) Structural drawings for CuNTA coordinated to two histidine residues (top) and the SLIM label (bottom). (B) Visualization of the labeled GB1 construct, with modeled dHis-CuNTA and SLIM rotamers[59] shown as sticks. (C) Simulated distance distribution obtained from Colab running mtsslWizard for bipedal labels.[35,59,60]

to the rigidity of this labeled side chain.[35,42,47−50] CuNTA increases specificity to dHis sites compared to free Cu^{II} in solution, which has a stronger propensity for unspecific binding.[42,47,51] Depending on the secondary structural elements (α-helix or β-sheet), dissociation constants (K_d) were determined to be on the order of 10^{-5} to 10^{-7} under EPR conditions.[49,52] An advantage of using spectroscopically orthogonal labels is that binding sites can be saturated by an excess of CuNTA without overlap with the detected signal.[52] Furthermore, the dHis-CuNTA labeling has been shown to be robust against competing ligands and to retain its high affinity binding over a wide pH range, thus demonstrating biologically relevant compatibility.[50] While a majority of the benchmarking studies on dHis-CuNTA have been performed on different constructs of a model protein (GB1, *vide infra*), this labeling approach has also been applied to a variety of more complex biological systems.[30,45,53] Despite its vulnerability to reduction, CuNTA has been used for in-cell PDS.[54]

Sensitivity is crucially important for the PDS studies. Over the past decade, the research questions investigated with PDS have involved ever larger biomolecular complexes.[19] It is conceivable that these are concentration-limited, due to either poor solubility or a low expression yield. Studying the dispersed state of proteins undergoing liquid−liquid phase separation at micromolar concentrations[55] requires submicromolar sensitivities. Furthermore, physiologically relevant conditions normally require high-sensitivity techniques due to the generally low concentrations of most biomolecules *in cellulo* or *in vivo*. Recent benchmarking studies have demonstrated that PDS allows measurements at nanomolar spin concentrations *in vitro* and in cell. In one study, spectroscopically orthogonal labeling using dHis-CuNTA and the nitroxide MTSL in combination with RIDME measurements yielded reliable distance information in the short-to-medium distance range down to a protein concentration of 100 nM *in vitro*,[6] and similar concentration limits were reported for *in vitro* nitroxide−nitroxide and in-cell Gd^{III}−Gd^{III} PELDOR measurements.[2] Recent studies reported DQC-based distance measurements at protein concentrations of 25 nM (short distance range) and 45 nM (long distance range) doubly labeled with MTSL[1] and oxSLIM, respectively.[3] At sufficiently low temperature and spin concentration, the electron spin dephasing time becomes independent of concentration,[56] and the achievable distance range is largely limited by deuteration levels of the sample.[4,57]

With the commonly used large volume resonators and rectangular pulses, one limiting factor for the sensitivity of nitroxides is the excitation bandwidth; here, labels with a narrow spectral line width such as trityls could entail a 3−4-fold increase in sensitivity by allowing excitation of the full spectrum. In this work, we benchmarked concentration sensitivities for spectroscopically orthogonal labeling using dHis-CuNTA[47] in combination with the trityl-based label SLIM[23] at standard Q-band (34 GHz) settings in a model protein. We hypothesized that by exchanging the nitroxide MTSL[6] with the trityl SLIM, and by employing the recently introduced variable-time RIDME experiment,[13] distance measurements in the low-nanomolar concentration regime should be feasible.

To enable direct comparison to some of the previous benchmarking studies,[5,6] dHis-CuNTA and SLIM were grafted onto the *Streptococcus* sp. group G protein G, B1 domain (GB1), an established model protein extensively used for EPR studies.[1,5,6,36,42,47,49,50,52,58] Here, the GB1 construct I6C/K28H/Q32H was used,[6,52] bearing the dHis motif for coordination to CuNTA in an α-helix and a cysteine residue for SLIM labeling in a β-sheet (Figure 1).

GB1 I6C/K28H/Q32H was expressed and purified as described previously[52] and labeled with SLIM and CuNTA according to established protocols (for more details, see the Supporting Information).[23,45,52] Quantitative labeling with SLIM could be achieved as demonstrated by sample characterization using continuous wave (CW) EPR spectroscopy (Figure S1), electrospray ionization (ESI) mass spectrometry (Figure S2), and ultraviolet−visible (UV−vis) spectroscopy (Figure S3) for concentration determination and estimation of labeling efficiency.

Initially, temperature optimization in the range of 30−70 K was performed by generating a temperature-dependent RIDME sensitivity profile (Figure S4 and Tables S2 and S3).[52] An optimum temperature of 40 K was determined for CuNTA-SLIM RIDME measurements, in agreement with a recent study.[45] Thus, compared to the CuNTA-nitroxide RIDME measured at 30 K,[52] here the unfavorable change in thermal polarization resulting from a 10 K increase in temperature was outweighed by a faster repetition rate with a higher temperature. With the repetition rate of the trityl (at 40 K in this study) and of the nitroxide (at 30 K)[6,52] being very similar, an overall increase in the sensitivity of the CuNTA-SLIM RIDME measurement will therefore be due to the excitation of the full spectral width of the trityl. Assuming that only approximately one-quarter to one-third of the nitroxide spectrum has been excited in previous CuNTA-nitroxide RIDME studies,[6,52] we hypothesized that an increase in

https://doi.org/10.1021/acs.jpclett.3c03311
J. Phys. Chem. Lett. 2024, 15, 1455−1461

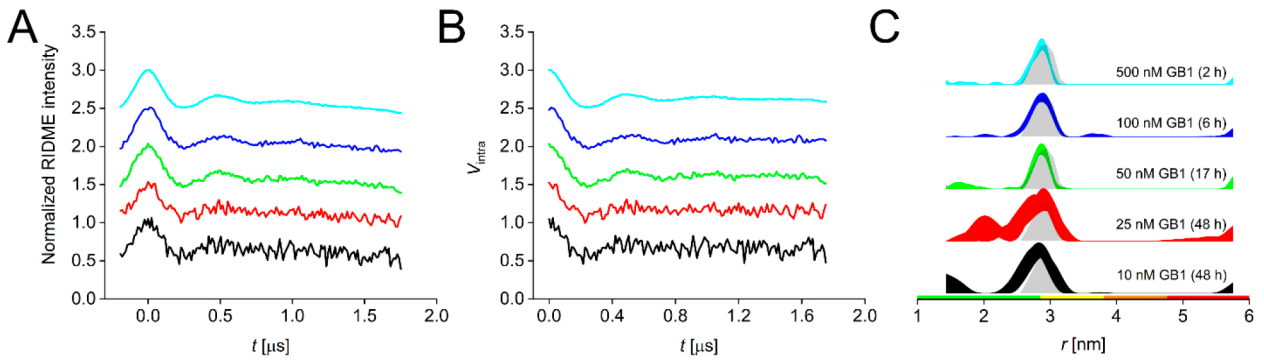

Figure 2. ctRIDME data for the GB1 I6SLIM/K28H/Q32H dilution series. (A) Stacked raw and (B) background-corrected RIDME traces for the 500 nM (cyan), 100 nM (blue), 50 nM (green), 25 nM (red), and 10 nM (black) samples. (C) Corresponding distance distributions given as 95% confidence estimates ($\pm 2\sigma$) with 50% noise added for error estimation during statistical analysis and simulated distance distributions shown as gray shaded areas. Color bars represent reliability ranges: green for shape reliable, yellow for mean and width reliable, orange for mean reliable, and red for no quantification possible.

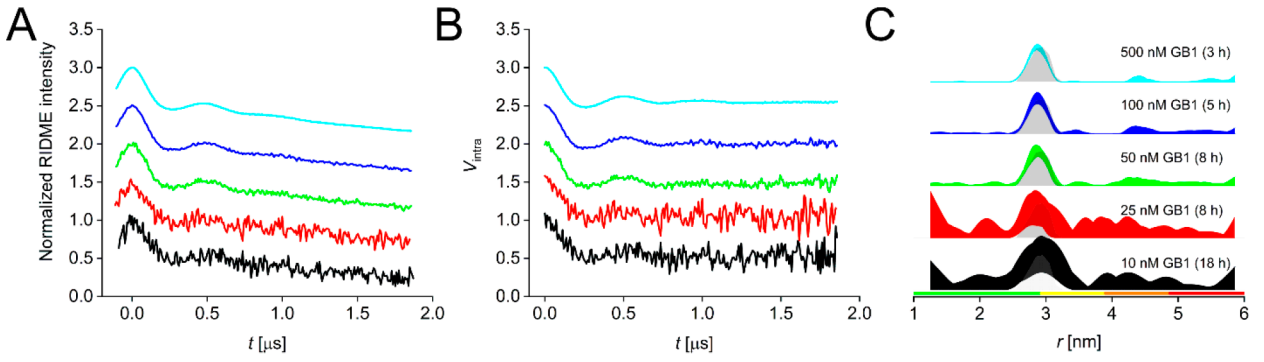

Figure 3. vtRIDME data for the GB1 I6SLIM/K28H/Q32H dilution series. (A) Stacked raw and (B) background-corrected RIDME traces for the 500 nM (cyan), 100 nM (blue), 50 nM (green), 25 nM (red), and 10 nM (black) samples. (C) Corresponding distance distributions given as 95% confidence estimates ($\pm 2\sigma$) with 50% noise added for error estimation during statistical analysis and simulated distance distributions shown as gray shaded areas. Color bars represent reliability ranges: green for shape reliable, yellow for mean and width reliable, orange for mean reliable, and red for no quantification possible.

sensitivity by a factor of 3−4 could be expected in an ideal case.

To test this hypothesis, a dilution series was set up, ranging from 500 nM to 10 nM protein, with the CuNTA concentration in each sample calculated to yield approximately 90% binding (Table S1).[52] Standard constant-time (ct) RIDME measurements were performed with identical experimental parameters for each sample, with the exception of the averaging times (and, thus, the number of scans) varying between 2 h for the 500 nM sample to ∼48 h for the 10 nM sample (Figure 2 and Figure S5).

ctRIDME data were processed using a Tikhonov regularization procedure within DeerAnalysis2022[61] as described previously,[6] and the obtained distance distributions for all samples were in excellent agreement with the simulated distribution. It should be noted that our in-house RIDME processing protocol follows a very conservative approach, potentially overestimating the uncertainty in the resulting distance distribution (for details, see the Supporting Information). While we obtained high-confidence distance distributions down to 50 nM protein, lower concentrations led to significantly increased uncertainties, including broader confidence bands, and such data should be interpreted only with great care.[4] Thus, concentrations of <50 nM remain a challenge for ctRIDME even when using CuNTA-SLIM label pairs, and higher-quality data with lower uncertainties than seen for 10 and 25 nM will be required to, e.g., determine whether multiple distance populations are present, as observed previously.[5] This is in line with data obtained from alternative deep neural network processing (DEERNet[62] with a RIDME background model[63] and ConsensusDeerAnalyzer2.0 within DeerAnalysis2022), which returned confirmative results for higher protein concentrations (Table S5) but failed for concentrations of ≲50 nM.

Data were also evaluated on the basis of their respective sensitivity values. Briefly, we define sensitivity as the ratio of modulation depth divided by the root-mean-square experimental noise; this modulation-to-noise ratio is further normalized as described previously,[5,6,52] thereby allowing a direct comparison of sensitivities obtained in different studies (see the Supporting Information for details on sensitivity analysis and tabulated values). Here, of particular interest was the direct sensitivity comparison to CuNTA-nitroxide ctRIDME measurements on the same GB1 construct that was used in this study (GB1 I6R1/K28H/Q32H, with R1 being the name of the side chain obtained from MTSL labeling of a cysteine residue) at protein concentrations of 50 and 100 nM.[6] As detailed above, the ability to excite the full width of the trityl EPR spectrum should lead to an increase in sensitivity of a factor of approximately 3−4 in an ideal case. Indeed, our

https://doi.org/10.1021/acs.jpclett.3c03311
J. Phys. Chem. Lett. 2024, 15, 1455−1461

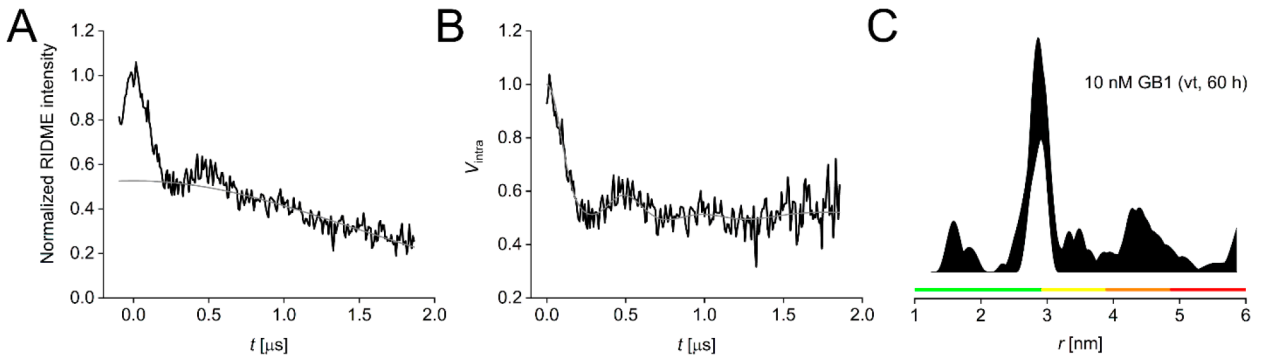

Figure 4. vtRIDME data for the 10 nM GB1 I6SLIM/K28H/Q32H sample averaged over 60 h. (A) Raw vtRIDME trace (black) with background (gray). (B) Background-corrected vtRIDME trace (black) and fit (gray). (C) Corresponding distance distribution given as the 95% confidence estimate ($\pm 2\sigma$) with 50% noise added for error estimation during statistical analysis. Color bars represent reliability ranges: green for shape reliable, yellow for mean and width reliable, orange for mean reliable, and red for no quantification possible.

data revealed an improvement of a factor of >3 (Table S4), and we were able to measure a 50 nM GB1 sample overnight (17 h) instead of averaging for ∼60 h;[6] we would refrain from using the data obtained at lower concentrations using ctRIDME due to the poor modulation-to-noise ratios achieved. The sensitivity comparison also identifies the 25 nM sample as an outlier of the series, with an extrapolated sensitivity of around half of the expected value, while the 100, 50, and 10 nM samples give values in good agreement with extrapolated values (see Table S4, column "S_t at 1 μM extrapolated").

In the next step, we investigated whether the recently reported variable-time RIDME experiment (vtRIDME)[13] would enable a further sensitivity increase particularly valuable at these low concentrations. To ensure reproducibility and minimize errors from sample positioning and experiment optimization, four experiments were recorded on the samples of the dilution series: a ctRIDME similar to the measurement described above, a vtRIDME with otherwise identical parameters, and corresponding reference traces for both the ctRIDME and the vtRIDME to enable deconvolution of the data (division by the reference trace).[52] Nondeconvoluted vtRIDME data are shown in Figure 3, and for a complete set of the ct/vtRIDME data, see Figure S6.

For the sake of convenience, the four different experiments have been combined into a single pulse program. For samples with a protein concentration of <100 nM, recording the reference traces became unfeasible due to the required extended averaging times and was therefore done only for concentrations of ≥100 nM. As observed previously,[13,35] modulation depths were slightly higher for the vtRIDME than for the ctRIDME. Deconvolution reduced the observed modulation depths for both ct- and vtRIDME measurements as expected. vtRIDME data were processed in the same way as described for the ctRIDME. Notably, here the additional processing with ConsensusDeerAnalyzer2.0 failed only for the lowest concentration (10 nM GB1) (Table S6), and a high-confidence distance distribution was obtained at 50 nM in 8 h. Sensitivity analysis revealed an approximately 2.5-fold increase in sensitivity for vtRIDME compared to ctRIDME (Table S4), which is in excellent agreement with recently published data.[13] While for the 50 nM vtRIDME a modulation-to-noise ratio of >20 was achieved with an averaging time of 8 h, the 25 and 10 nM samples yielded ratios of <10 with averaging times of 8 and 18 h, respectively; data of this quality should not be used to interpret distance distributions.[4] Thus, together with the change from CuNTA-nitroxide to CuNTA-SLIM labeling, an overall increase in sensitivity of almost an order of magnitude (∼8-fold) compared to the previous study[6] has been achieved.

Finally, to demonstrate that 10 nM measurements can be recorded at sufficient quality, we averaged a vtRIDME experiment of the 10 nM GB1 sample for approximately 60 h, our internal maximum averaging time used for previous sensitivity benchmarking,[6] which yielded clearly visible oscillations, and a modulation-to-noise ratio of 12.5 (Figure 4). While this is below the recent recommendation of a modulation-to-noise ratio of at least 20, these data are still of sufficient quality to provide useful structural restraints.[4] An attempt to further decrease the protein concentration to 5 nM for a vtRIDME measurement turned out to be beyond our current sensitivity limit and was considered unsuitable for processing (Figure S7).

In summary, we show that combining CuNTA-SLIM spin-labeling with vtRIDME can significantly enhance PDS sensitivity by almost an order of magnitude compared to established procedures (i.e., ctRIDME measurement of CuNTA-nitroxide-labeled protein), reaching a concentration limit of 10 nM in the distance range of 3 nm. It is expected that longer distances and broader or more complex distributions will require longer dipolar evolution times or a better modulation-to-noise ratio. This would likely demand concentrations higher than those achieved here. Together with recent advances in hardware,[1,64] we predict that single-digit nanomolar PDS distance measurements will soon be within reach in favorable cases. This will enable new science, particularly with respect to concentration-limited systems.

■ ASSOCIATED CONTENT

Data Availability Statement

The research data supporting this publication will be accessible at 10.17630/4a648038-3e79-4eaf-a185-f6721e4060fa.[65]

Supporting Information

The Supporting Information is available free of charge at https://pubs.acs.org/doi/10.1021/acs.jpclett.3c03311.

Protein expression, purification, and spin-labeling; continuous wave (CW) EPR, mass spectrometry, and UV−vis data; EPR sample preparation and temperature optimization for RIDME; RIDME measurements and data processing and analysis; modeling; sensitivity

https://doi.org/10.1021/acs.jpclett.3c03311
J. Phys. Chem. Lett. 2024, 15, 1455−1461

considerations; supplementary RIDME data and CDA2.0 report; and references and author contributions (PDF)

Transparent Peer Review report available (PDF)

AUTHOR INFORMATION

Corresponding Authors

Olav Schiemann − *Clausius-Institute of Physical and Theoretical Chemistry, University of Bonn, 53115 Bonn, Germany*; orcid.org/0000-0001-6346-9779; Email: schiemann@pc.uni-bonn.de

Bela E. Bode − *EaStCHEM School of Chemistry and Biomedical Sciences Research Complex, Centre of Magnetic Resonance, University of St Andrews, St Andrews KY16 9ST, U.K.*; orcid.org/0000-0002-3384-271X; Email: beb2@st-andrews.ac.uk

Authors

Katrin Ackermann − *EaStCHEM School of Chemistry and Biomedical Sciences Research Complex, Centre of Magnetic Resonance, University of St Andrews, St Andrews KY16 9ST, U.K.*; orcid.org/0000-0003-1632-0503

Caspar A. Heubach − *Clausius-Institute of Physical and Theoretical Chemistry, University of Bonn, 53115 Bonn, Germany*

Complete contact information is available at: https://pubs.acs.org/10.1021/acs.jpclett.3c03311

Notes

The authors declare no competing financial interest.

ACKNOWLEDGMENTS

To meet institutional and research funder open access requirements, any accepted manuscript arising shall be open access under a Creative Commons Attribution (CC BY) reuse licence with zero embargo. The authors acknowledge support by a University of St Andrews-University of Bonn Collaborative Research Grant, by the Wellcome Trust (204821/Z/16/Z), and by the EPSRC (EP/X016455/1). B.E.B. acknowledges equipment funding by BBSRC (BB/R013780/1 and BB/T017740/1). O.S. thanks the DFG for funding (420322655). C.A.H. thanks the DAAD for a travel and research scholarship. The authors thank the StAnD (St Andrews and Dundee) EPR grouping for long-standing support and the St Andrews mass spectrometry and proteomics facility for equipment access.

REFERENCES

(1) Mandato, A.; Hasanbasri, Z.; Saxena, S. Double Quantum Coherence ESR at Q-Band Enhances the Sensitivity of Distance Measurements at Submicromolar Concentrations. *J. Phys. Chem. Lett.* **2023**, *14*, 8909−8915.

(2) Kucher, S.; Elsner, C.; Safonova, M.; Maffini, S.; Bordignon, E. In-Cell Double Electron−Electron Resonance at Nanomolar Protein Concentrations. *J. Phys. Chem. Lett.* **2021**, *12*, 3679−3684.

(3) Fleck, N.; Heubach, C.; Hett, T.; Spicher, S.; Grimme, S.; Schiemann, O. Ox-SLIM: Synthesis of and Site-Specific Labelling with a Highly Hydrophilic Trityl Spin Label. *Chem. - Eur. J.* **2021**, *27*, 5292−5297.

(4) Schiemann, O.; Heubach, C. A.; Abdullin, D.; Ackermann, K.; Azarkh, M.; Bagryanskaya, E. G.; Drescher, M.; Endeward, B.; Freed, J. H.; Galazzo, L.; Goldfarb, D.; Hett, T.; Esteban Hofer, L.; Fábregas Ibáñez, L.; Hustedt, E. J.; Kucher, S.; Kuprov, I.; Lovett, J. E.; Meyer, A.; Ruthstein, S.; Saxena, S.; Stoll, S.; Timmel, C. R.; Di Valentin, M.; McHaourab, H. S.; Prisner, T. F.; Bode, B. E.; Bordignon, E.; Bennati, M.; Jeschke, G. Benchmark Test and Guidelines for DEER/PELDOR Experiments on Nitroxide-Labeled Biomolecules. *J. Am. Chem. Soc.* **2021**, *143*, 17875−17890.

(5) Ackermann, K.; Wort, J. L.; Bode, B. E. Nanomolar Pulse Dipolar EPR Spectroscopy in Proteins: Cu^{II}−Cu^{II} and Nitroxide−Nitroxide Cases. *J. Phys. Chem. B* **2021**, *125*, 5358−5364.

(6) Ackermann, K.; Wort, J. L.; Bode, B. E. Pulse Dipolar EPR for Determining Nanomolar Binding Affinities. *Chem. Commun.* **2022**, *58*, 8790−8793.

(7) Martin, R. E.; Pannier, M.; Diederich, F.; Gramlich, V.; Hubrich, M.; Spiess, H. W. Determination of End-to-End Distances in a Series of TEMPO Diradicals of up to 2.8 nm Length with a New Four-Pulse Double Electron Electron Resonance Experiment. *Angew. Chem., Int. Ed.* **1998**, *37*, 2833−2837.

(8) Milov, A. D.; Salikov, K. M.; Shirov, M. D. Application of ELDOR in Electron-Spin Echo for Paramagnetic Center Space Distribution in Solids. *Fiz. Tverd. Tela* **1981**, *23*, 975−982.

(9) Pannier, M.; Veit, S.; Godt, A.; Jeschke, G.; Spiess, H. W. Dead-Time Free Measurement of Dipole-Dipole Interactions between Spins. *J. Magn. Reson.* **2000**, *142*, 331−340.

(10) Kulik, L. V.; Dzuba, S. A.; Grigoryev, I. A.; Tsvetkov, Y. D. Electron Dipole−Dipole Interaction in ESEEM of Nitroxide Biradicals. *Chem. Phys. Lett.* **2001**, *343*, 315−324.

(11) Milikisyants, S.; Scarpelli, F.; Finiguerra, M. G.; Ubbink, M.; Huber, M. A Pulsed EPR Method to Determine Distances Between Paramagnetic Centers with Strong Spectral Anisotropy and Radicals: The Dead-time Free RIDME Sequence. *J. Magn. Reson.* **2009**, *201*, 48−56.

(12) Abdullin, D.; Suchatzki, M.; Schiemann, O. Six-Pulse RIDME Sequence to Avoid Background Artifacts. *Appl. Magn. Reson.* **2022**, *53*, 539−554.

(13) Wort, J. L.; Ackermann, K.; Giannoulis, A.; Bode, B. E. Enhanced sensitivity for pulse dipolar EPR spectroscopy using variable-time RIDME. *J. Magn. Reson.* **2023**, *352*, No. 107460.

(14) Abdullin, D.; Duthie, F.; Meyer, A.; Müller, E. S.; Hagelueken, G.; Schiemann, O. Comparison of PELDOR and RIDME for Distance Measurements between Nitroxides and Low-Spin Fe(III) Ions. *J. Phys. Chem. B* **2015**, *119*, 13534−13542.

(15) Saxena, S.; Freed, J. H. Double Quantum Two-Dimensional Fourier Transform Electron Spin Resonance: Distance Measurements. *Chem. Phys. Lett.* **1996**, *251*, 102−110.

(16) Bowman, A.; Hammond, C. M.; Stirling, A.; Ward, R.; Shang, W.; El-Mkami, H.; Robinson, D. A.; Svergun, D. I.; Norman, D. G.; Owen-Hughes, T. The Histone Chaperones Vps75 and Nap1 Form Ring-Like, Tetrameric Structures in Solution. *Nucleic Acids Res.* **2014**, *42*, 6038−6051.

(17) Jeschke, G. DEER Distance Measurements on Proteins. *Annu. Rev. Phys. Chem.* **2012**, *63*, 419−446.

(18) Schmidt, T.; Wälti, M. A.; Baber, J. L.; Hustedt, E. J.; Clore, G. M. Long Distance Measurements up to 160 Å in the GroEL Tetradecamer Using Q-Band DEER EPR Spectroscopy. *Angew. Chem., Int. Ed.* **2016**, *55*, 15905−15909.

(19) Galazzo, L.; Bordignon, E. Electron Paramagnetic Resonance Spectroscopy in Structural-Dynamic Studies of Large Protein Complexes. *Prog. Nucl. Magn. Reson. Spectrosc.* **2023**, *134*−*135*, 1−19.

(20) Jeschke, G. The Contribution of Modern EPR to Structural Biology. *Emerging Topics in Life Sciences* **2018**, *2*, 9−18.

(21) Azarkh, M.; Bieber, A.; Qi, M.; Fischer, J. W. A.; Yulikov, M.; Godt, A.; Drescher, M. Gd(III)-Gd(III) Relaxation-Induced Dipolar Modulation Enhancement for In-Cell Electron Paramagnetic Resonance Distance Determination. *J. Phys. Chem. Lett.* **2019**, *10*, 1477−1481.

(22) Duss, O.; Michel, E.; Yulikov, M.; Schubert, M.; Jeschke, G.; Allain, F. H. T. Structural Basis of the Non-Coding RNA RsmZ Acting as a Protein Sponge. *Nature* **2014**, *509*, 588−592.

(23) Fleck, N.; Heubach, C. A.; Hett, T.; Haege, F. R.; Bawol, P. P.; Baltruschat, H.; Schiemann, O. SLIM: A Short-Linked, Highly Redox-Stable Trityl Label for High-Sensitivity In-Cell EPR Distance Measurements. *Angew. Chem., Int. Ed.* **2020**, *59*, 9767−9772.

(24) Hagelueken, G.; Ingledew, W. J.; Huang, H.; Petrovic-Stojanovska, B.; Whitfield, C.; ElMkami, H.; Schiemann, O.; Naismith, J. H. PELDOR Spectroscopy Distance Fingerprinting of the Octameric Outer-Membrane Protein Wza from *Escherichia coli*. *Angew. Chem., Int. Ed.* **2009**, *48*, 2904−2906.
(25) Igarashi, R.; Sakai, T.; Hara, H.; Tenno, T.; Tanaka, T.; Tochio, H.; Shirakawa, M. Distance Determination in Proteins inside *Xenopus laevis* Oocytes by Double Electron−Electron Resonance Experiments. *J. Am. Chem. Soc.* **2010**, *132*, 8228−8229.
(26) Jassoy, J. J.; Berndhäuser, A.; Duthie, F.; Kühn, S. P.; Hagelueken, G.; Schiemann, O. Versatile Trityl Spin Labels for Nanometer Distance Measurements on Biomolecules In Vitro and within Cells. *Angew. Chem., Int. Ed.* **2017**, *56*, 177−181.
(27) Joseph, B.; Sikora, A.; Bordignon, E.; Jeschke, G.; Cafiso, D. S.; Prisner, T. F. Distance Measurement on an Endogenous Membrane Transporter in *E. coli* Cells and Native Membranes Using EPR Spectroscopy. *Angew. Chem., Int. Ed.* **2015**, *54*, 6196−6199.
(28) Kapsalis, C.; Wang, B.; El Mkami, H.; Pitt, S. J.; Schnell, J. R.; Smith, T. K.; Lippiat, J. D.; Bode, B. E.; Pliotas, C. Allosteric Activation of an Ion Channel Triggered by Modification of Mechanosensitive Nano-Pockets. *Nat. Commun.* **2019**, *10*, 4619.
(29) Krstić, I.; Hänsel, R.; Romainczyk, O.; Engels, J. W.; Dötsch, V.; Prisner, T. F. Long-Range Distance Measurements on Nucleic Acids in Cells by Pulsed EPR Spectroscopy. *Angew. Chem., Int. Ed.* **2011**, *50*, 5070−5074.
(30) Sameach, H.; Ghosh, S.; Gevorkyan-Airapetov, L.; Saxena, S.; Ruthstein, S. EPR Spectroscopy Detects Various Active State Conformations of the Transcriptional Regulator CueR. *Angew. Chem., Int. Ed.* **2019**, *58*, 3053−3056.
(31) Verhalen, B.; Dastvan, R.; Thangapandian, S.; Peskova, Y.; Koteiche, H. A.; Nakamoto, R. K.; Tajkhorshid, E.; McHaourab, H. S. Energy Transduction and Alternating Access of the Mammalian ABC Transporter P-Glycoprotein. *Nature* **2017**, *543*, 738−741.
(32) Yang, Z.; Liu, Y.; Borbat, P.; Zweier, J. L.; Freed, J. H.; Hubbell, W. L. Pulsed ESR Dipolar Spectroscopy for Distance Measurements in Immobilized Spin Labeled Proteins in Liquid Solution. *J. Am. Chem. Soc.* **2012**, *134*, 9950−9952.
(33) Berliner, L. J.; Grunwald, J.; Hankovszky, H. O.; Hideg, K. A Novel Reversible Thiol-Specific Spin Label: Papain Active Site Labeling and Inhibition. *Anal. Biochem.* **1982**, *119*, 450−455.
(34) Gmeiner, C.; Klose, D.; Mileo, E.; Belle, V.; Marque, S. R. A.; Dorn, G.; Allain, F. H. T.; Guigliarelli, B.; Jeschke, G.; Yulikov, M. Orthogonal Tyrosine and Cysteine Site-Directed Spin Labeling for Dipolar Pulse EPR Spectroscopy on Proteins. *J. Phys. Chem. Lett.* **2017**, *8*, 4852−4857.
(35) Vitali, V.; Ackermann, K.; Hagelueken, G.; Bode, B. E. Spectroscopically Orthogonal Labelling to Disentangle Site-Specific Nitroxide Label Distributions. *Appl. Magn. Reson.* **2023**, DOI: 10.1007/s00723-023-01611-1.
(36) Giannoulis, A.; Yang, Y.; Gong, Y.-J.; Tan, X.; Feintuch, A.; Carmieli, R.; Bahrenberg, T.; Liu, Y.; Su, X.-C.; Goldfarb, D. DEER Distance Measurements on Trityl/Trityl and Gd(III)/Trityl Labelled Proteins. *Phys. Chem. Chem. Phys.* **2019**, *21*, 10217−10227.
(37) Galazzo, L.; Meier, G.; Timachi, M. H.; Hutter, C. A. J.; Seeger, M. A.; Bordignon, E. Spin-Labeled Nanobodies as Protein Conformational Reporters for Electron Paramagnetic Resonance in Cellular Membranes. *Proc. Natl. Acad. Sci. U.S.A.* **2020**, *117*, 2441−2448.
(38) Razzaghi, S.; Qi, M.; Nalepa, A. I.; Godt, A.; Jeschke, G.; Savitsky, A.; Yulikov, M. RIDME Spectroscopy with Gd(III) Centers. *J. Phys. Chem. Lett.* **2014**, *5*, 3970−3975.
(39) Shah, A.; Roux, A.; Starck, M.; Mosely, J. A.; Stevens, M.; Norman, D. G.; Hunter, R. I.; El Mkami, H.; Smith, G. M.; Parker, D.; Lovett, J. E. A Gadolinium Spin Label with Both a Narrow Central Transition and Short Tether for Use in Double Electron Electron Resonance Distance Measurements. *Inorg. Chem.* **2019**, *58*, 3015−3025.
(40) Giannoulis, A.; Feintuch, A.; Barak, Y.; Mazal, H.; Albeck, S.; Unger, T.; Yang, F.; Su, X.-C.; Goldfarb, D. Two Closed ATP- and ADP-Dependent Conformations in Yeast Hsp90 Chaperone Detected by Mn(II) EPR Spectroscopic Techniques. *Proc. Natl. Acad. Sci. U.S.A.* **2020**, *117*, 395−404.
(41) Abdullin, D.; Schiemann, O. Pulsed Dipolar EPR Spectroscopy and Metal Ions: Methodology and Biological Applications. *ChemPlusChem.* **2020**, *85*, 353−372.
(42) Cunningham, T. F.; Putterman, M. R.; Desai, A.; Horne, W. S.; Saxena, S. The Double-Histidine Cu^{2+}-Binding Motif: a Highly Rigid, Site-Specific Spin Probe for Electron Spin Resonance Distance Measurements. *Angew. Chem., Int. Ed.* **2015**, *54*, 6330−6334.
(43) Ghosh, S.; Lawless, M. J.; Brubaker, H. J.; Singewald, K.; Kurpiewski, M. R.; Jen-Jacobson, L.; Saxena, S. Cu^{2+}-Based Distance Measurements by Pulsed EPR Provide Distance Constraints for DNA Backbone Conformations in Solution. *Nucleic Acids Res.* **2020**, *48*, e49−e49.
(44) Stratmann, L. M.; Kutin, Y.; Kasanmascheff, M.; Clever, G. H. Precise Distance Measurements in DNA G-Quadruplex Dimers and Sandwich Complexes by Pulsed Dipolar EPR Spectroscopy. *Angew. Chem., Int. Ed.* **2021**, *60*, 4939.
(45) Heubach, C. A.; Hasanbasri, Z.; Abdullin, D.; Reuter, A.; Korzekwa, B.; Saxena, S.; Schiemann, O. Differentiating between Label and Protein Conformers in Pulsed Dipolar EPR Spectroscopy with the dHis-Cu^{2+}(NTA) Motif. *Chem. - Eur. J.* **2023**, *29*, No. e202302541.
(46) Ackermann, K.; Chapman, A.; Bode, B. E. A Comparison of Cysteine-Conjugated Nitroxide Spin Labels for Pulse Dipolar EPR Spectroscopy. *Molecules* **2021**, *26*, 7534.
(47) Ghosh, S.; Lawless, M. J.; Rule, G. S.; Saxena, S. The Cu^{2+}-Nitrilotriacetic Acid Complex Improves Loading of α-Helical Double Histidine Site for Precise Distance Measurements by Pulsed ESR. *J. Magn. Reson.* **2018**, *286*, 163−171.
(48) Ghosh, S.; Saxena, S.; Jeschke, G. Rotamer Modelling of Cu(II) Spin Labels Based on the Double-Histidine Motif. *Appl. Magn. Reson.* **2018**, *49*, 1281−1298.
(49) Wort, J. L.; Ackermann, K.; Norman, D. G.; Bode, B. E. A General Model to Optimise Cu^{II} Labelling Efficiency of Double-Histidine Motifs for Pulse Dipolar EPR Applications. *Phys. Chem. Chem. Phys.* **2021**, *23*, 3810−3819.
(50) Wort, J. L.; Arya, S.; Ackermann, K.; Stewart, A. J.; Bode, B. E. Pulse Dipolar EPR Reveals Double-Histidine Motif Cu^{II}−NTA Spin-Labeling Robustness against Competitor Ions. *J. Phys. Chem. Lett.* **2021**, *12*, 2815−2819.
(51) Ackermann, K.; Khazaipoul, S.; Wort, J. L.; Sobczak, A. I. S.; Mkami, H. E.; Stewart, A. J.; Bode, B. E. Investigating Native Metal Ion Binding Sites in Mammalian Histidine-Rich Glycoprotein. *J. Am. Chem. Soc.* **2023**, *145*, 8064−8072.
(52) Wort, J. L.; Ackermann, K.; Giannoulis, A.; Stewart, A. J.; Norman, D. G.; Bode, B. E. Sub-Micromolar Pulse Dipolar EPR Spectroscopy Reveals Increasing Cu^{II}-labelling of Double-Histidine Motifs with Lower Temperature. *Angew. Chem., Int. Ed.* **2019**, *58*, 11681−11685.
(53) Bogetti, X.; Bogetti, A.; Casto, J.; Rule, G.; Chong, L.; Saxena, S. Direct Observation of Negative Cooperativity in a Detoxification Enzyme at the Atomic Level by Electron Paramagnetic Resonance spectroscopy and Simulation. *Protein Sci.* **2023**, *32*, No. e4770.
(54) Shenberger, Y.; Gevorkyan-Airapetov, L.; Hirsch, M.; Hofmann, L.; Ruthstein, S. An in-Cell Spin-Labelling Methodology Provides Structural Information on Cytoplasmic Proteins in Bacteria. *Chem. Commun.* **2023**, *59*, 10524−10527.
(55) Harami, G. M.; Kovács, Z. J.; Pancsa, R.; Pálinkás, J.; Baráth, V.; Tárnok, K.; Málnási-Csizmadia, A.; Kovács, M. Phase Separation by ssDNA Binding Protein Controlled via Protein−Protein and Protein−DNA Interactions. *Proc. Natl. Acad. Sci. U.S.A.* **2020**, *117*, 26206−26217.
(56) Dastvan, R.; Bode, B. E.; Karuppiah, M. P. R.; Marko, A.; Lyubenova, S.; Schwalbe, H.; Prisner, T. F. Optimization of Transversal Relaxation of Nitroxides for Pulsed Electron−Electron Double Resonance Spectroscopy in Phospholipid Membranes. *J. Phys. Chem. B* **2010**, *114*, 13507−13516.

(57) Ward, R.; Bowman, A.; Sozudogru, E.; El-Mkami, H.; Owen-Hughes, T.; Norman, D. G. EPR Distance Measurements in Deuterated Proteins. *J. Magn. Reson.* **2010**, *207*, 164−167.
(58) Gamble Jarvi, A.; Ranguelova, K.; Ghosh, S.; Weber, R. T.; Saxena, S. On the Use of Q-Band Double Electron−Electron Resonance To Resolve the Relative Orientations of Two Double Histidine-Bound Cu^{2+} Ions in a Protein. *J. Phys. Chem. B* **2018**, *122*, 10669−10677.
(59) https://colab.research.google.com/github/gha2012/mtsslWizard_colab/blob/main/mtsslWizard_colab.ipynb (accessed 2023-09-25).
(60) Hagelueken, G.; Ward, R.; Naismith, J. H.; Schiemann, O. MtsslWizard: In Silico Spin-Labeling and Generation of Distance Distributions in PyMOL. *Appl. Magn. Reson.* **2012**, *42*, 377−391.
(61) Jeschke, G.; Chechik, V.; Ionita, P.; Godt, A.; Zimmermann, H.; Banham, J.; Timmel, C. R.; Hilger, D.; Jung, H. DeerAnalysis2006 - a Comprehensive Software Package for Analyzing Pulsed ELDOR Data. *Appl. Magn. Reson.* **2006**, *30*, 473−498.
(62) Worswick, S. G.; Spencer, J. A.; Jeschke, G.; Kuprov, I. Deep Neural Network Processing of DEER Data. *Sci. Adv.* **2018**, *4*, No. eaat5218.
(63) Keeley, J.; Choudhury, T.; Galazzo, L.; Bordignon, E.; Feintuch, A.; Goldfarb, D.; Russell, H.; Taylor, M. J.; Lovett, J. E.; Eggeling, A.; Fábregas Ibáñez, L.; Keller, K.; Yulikov, M.; Jeschke, G.; Kuprov, I. Neural Networks in Pulsed Dipolar Spectroscopy: A Practical Guide. *J. Magn. Reson.* **2022**, *338*, No. 107186.
(64) Šimėnas, M.; O'Sullivan, J.; Zollitsch, C. W.; Kennedy, O.; Seif-Eddine, M.; Ritsch, I.; Hülsmann, M.; Qi, M.; Godt, A.; Roessler, M. M.; Jeschke, G.; Morton, J. J. L. A Sensitivity Leap for X-Band EPR Using a Probehead with a Cryogenic Preamplifier. *J. Magn. Reson.* **2021**, *322*, No. 106876.
(65) Ackermann, K.; Heubach, C.; Schiemann, O.; Bode, B. E. Pulse Dipolar Electron Paramagnetic Resonance Spectroscopy Distance Measurements at Low Nanomolar Concentrations: The Cu^{II}-Trityl Case. Data set, 2024.

https://doi.org/10.1021/acs.jpclett.3c03311
J. Phys. Chem. Lett. 2024, 15, 1455−1461